Trop J Nat Prod Res, October 2020; 4(10):714-721 **ISSN 2616-0684 (Print)**
ISSN 2616-0692 (Electronic)

Tropical Journal of Natural Product Research

Available online at https://www.tjnpr.org

Original Research Article

Green Silver Nanoparticles Based on the Chemical Constituents of *Glinus lotoides* L.: *In Vitro* Anticancer and Antiviral Evaluation

Mai M. Farid[1], Mahmoud Emam[1,2], Reda S. Mohammed[3], Sameh R. Hussein[1], Mona M. Marzouk[1]*

[1]*Phytochemistry and Plant Systematics Department, National Research Centre, 33 El Bohouth St., Dokki, Giza, P.O. 12622, Egypt*
[2]*College of Pharmaceutical Science & Collaborative Innovation Center of Yangtze River Delta Region Green Pharmaceuticals, Zhejiang University of Technology, Hangzhou 310014, China*
[3]*Department of Pharmacognosy, National Research Centre, 33 El Bohouth St., Dokki, Giza, P.O. 12622, Egypt*

ARTICLE INFO

Article history:
Received 21 August 2020
Revised 28 September 2020
Accepted 27 October 2020
Published online 02 November 2020

ABSTRACT

Green silver nanoparticles (AgNPs) utilize companionable nanomaterials for investigative and therapeutic determinations. The existing study reports the synthesis of AgNPs using *Glinus lotoides* L. aqueous methanol extract (GLE) besides evaluation of anticancer and antiviral effects of GLE and its synthesized AgNPs (GLE_AgNPs). The formation of GLE_AgNPs was confirmed by UV-VIS spectrophotometer. Their spherical shape with average size was found to be 5-50 nm by TEM (transmission electron microscope). Fourier-transform infrared spectrometer (FTIR) investigation specified the presence of alcohol/phenol, amino and aromatic carbonyl groups in GLE that were complex in reduction and capping of nanoparticles. The *in vitro* cytotoxic activity of GLE was screened using four human carcinoma cell lines; liver (HepG2), colon (HCT116), breast (MCF7), larynx (Hep 2) and showed IC_{50} 24.3, 26.1, 30, 50 (µg/mL), compared to doxorubicin with IC_{50} 4.28, 3.73, 4.43, 3.73 (µg/mL), respectively. Furthermore, the antiproliferative effects (IC_{50}, µg/mL) of GLE_AgNPs were observed with HepG2 (25.4) and HCT116 (26.3) also it exhibited no cytotoxicity against normal human melanocytes (HFB-4). The antiviral activity showed a higher potency of GLE_AgNPs against H5N1 virus with inhibitory effect about 60%, while the GLE about 26.5% (100µg/µL). Additionally, the phytochemical constituents of GLE, which could be used as reducing agents in GLE_AgNPs, were characterized using spectrometric techniques. GC/MS analysis of the petroleum ether/dichloromethane fraction (1:1 *v/v*) revealed the identification of 33 compounds of fatty acids, fatty acid esters and sterols. LC/ESI/MS^n of the defatted GLE afforded 30 compounds that belong to phenolics, organic acids, flavonol *O*-glycosides, flavonol *O*-acyl glycosides and *C*-glycosyl flavonoids.

Keywords: *Glinus lotoides*, Silver nanoparticles, Antiviral, Cytotoxicity, GC/MS, LC/ESI/MS^n

Introduction

Green silver nanoparticles (AgNPs) are one of the furthermost effective symbols of nanoparticles that are being functional in many areas of life comprising therapeutic applications, water filter, food packaging, cosmetics, tumor imaging, and drug delivery.[1] AgNPs have increased great attention as nonhazardous, eco-friendly, cost-effective and simple progressive to predictable chemical methods.[2-6] Numerous *in vitro* studies using AgNPs have demonstrated their prospective as effective antimicrobial,[5,7] anticancer [8, 9] and antiviral agents.[10-12]

As well, the plant kingdom considered as unlimited resources for the expansion of unique bioactive agents along with different medicinal systems. The wild plant of *Glinus lotoides* L. (Family: Molluginaceae), recognized as lotus sweet juice and localized mostly in Egypt, Sudan, India, Pakistan and South Africa, and considered a promising dietary vegetable and medicinal plant.[13] In Egypt, it is used in folk medicine as a stomachic, stimulant and cardiac drug. The members of family Molluginaceae are mainly characterized by the presence of flavonols and *C*-glycosyl flavonoids. *G. lotoides* was reported to contain various saponin and triterpenoid derivatives.[14-16] *C*-glycosyl flavones (vitexin-2″-*O*-glucoside and vicenin-2) were also stated in the plant.[16] *G. lotoides* has numerous pharmacological activities including antitumor, anti-spasmodic, anti-helminthic, geno-toxic and bio-pesticidal activities. In Ethiopia, the crude extract of *G. lotoides* has been prepared in the form of tablet to be used for therapeutic purposes.[16]

In the current study, the aqueous methanol extract of *G. lotoides* (GLE) and its biosynthesized silver nanoparticles (AgNPs) were subjected to the anticancer evaluation against four human carcinoma cell lines (liver; HepG2, colon; HCT116, breast; MCF7 and larynx; Hep2) and the antiviral assessment against avian influenza A virus (H5N1). Moreover, the chemical analysis of GLE was characterized using mass spectrometric methods.

Materials and Methods

Plant material

G. lotoides whole plant was collected by Prof. Dr. Sameh R. Hussein from Giza cultivated areas in March 2016. A voucher specimen (No. sn SR/2358) was identified and deposited in the National Research Centre herbarium (CAIRC), Cairo, Egypt.

*Corresponding author. E mail: monakhalil66@hotmail.com
Tel: +01000970022

Citation: Farid MM, Emam M, Mohammed RS, Hussein SR, Marzouk MM. Green Silver Nanoparticles Based on the Chemical Constituents of *Glinus lotoides* L.: *In Vitro* Anticancer and Antiviral Evaluation. Trop J Nat Prod Res. 2020; 4(10):714-721. doi.org/10.26538/tjnpr/v4i10.10

Official Journal of Natural Product Research Group, Faculty of Pharmacy, University of Benin, Benin City, Nigeria.

ISSN 2616-0684 (Print)
ISSN 2616-0692 (Electronic)

Plant extract preparation

The dried, powdered aerial whole plant of *G. lotoides* (80 g) were extracted by (7:3 *v/v*) methanol/water and yielded 25 g of aqueous methanol extract of *G. lotoides* (GLE). A part of GLE was used for the AgNPs biosynthesis and the biological assay. The rest GLE was defatted with petroleum ether: dichloromethane (1:1 *v/v*). The petroleum ether: dichloromethane fraction and the defatted GLE kept at 4°C until use for phytochemical analysis.

Bio-synthesis of AgNPs and characterization of biosynthesized AgNPs

Silver nitrate ($AgNO_3$, Merck) were prepared by the reduction of 10 mL of aqueous $AgNO_3$ solution (1 mM) with different concentration of GLE at room temperature. The mixture was hand shaken and allowed to stand in the dark at room temperature. To study the effect of extract quantity on Ag NPs synthesis, the quantity was varied from 100 µL to 500 µL per 10 mL of silver nitrate solution (1 mM). The concentration of the $AgNO_3$ was still constant over the process (1mM), while the extract concentration changed, to investigate its effect upon the reduction, size of the biosynthesized nanoparticles. The obtained nanoparticle solution was purified by repeated centrifugation at 10,000 rpm for 20 min followed by re-dispersion of the pellet in deionized water. This process was repeated twice to isolate the pure AgNPs and exclude the presence of any unbound plant extract residue. The UV-vis spectra measurements were recorded using UV-2401 (PC) S, UV-Vis recording spectrophotometer (Shimadzu, Japan). The shape and sizes of the prepared samples were performed using transmission electron microscope (TEM) (JEOL-JEM-1011, Japan). The different kinds of the prepared AgNPs functional groups were characterized by using Fourier-transform infrared spectrometer **(** FTIR 4100 JASCO, Japan) in the range of 4000–400 cm^{-1}.[17]

In vitro anticancer assay

Human tumor cell lines; epidermal carcinoma of liver (HepG2), larynx (Hep2), colon (HCT116) and breast (MCF7) as well as normal human melanocytes (HFB-4) were obtained from the American Type Culture Collection (ATCC, Minisota, U.S.A.). The cell lines were maintained at the National Cancer Institute, Cairo, Egypt, by serial sub-culturing. The samples were prepared by dissolving Stock solution in dimethylsulfoxide (DMSO) at a concentration 100 mM and stored at -20°C. Their cytotoxic activities were carried out using SRB (Sulphorhodamine-B) assay following the method reported by Vichai and Kirtikara. [18] The relation between surviving fraction and samples concentration was plotted to obtain the survival curve of each tumor cell line as compared with Doxorubcin; the control anticancer drug.

In vitro antiviral assay

Madin-Darby Canine Kidney (MDCK) cells were obtained from the center of scientific excellence for influenza viruses, National Research Centre. The used highly pathogenic avian influenza (HPAI) virus A/Chicken/Egypt/M7217B/2013 (H5N1) was isolated in 2013 from the infected chickens in Egypt. The samples cytotoxic activities were tested in MDCK cells by using the MTT method, [19] the % cytotoxicity compared to the untreated cells was determined with the following equation: % Cytotoxicity= [(Abs of cell without treatment-Abs of cell with treatment)/Abs of cell without treatment] x 100, Abs**:** Absorbance (nm). Plaque reduction assay was used to determine the antiviral activity for GLE and AgNPs at safe concentrations. [20]

Phytochemical analysis

Acid hydrolysis and paper chromatography

The acid hydrolysis of 100 mg of the defatted GLE was achieved and investigated using paper chromatography for the ethyl acetate fraction to detect aglycones and the aqueous fraction to detect sugars, comparing with authentic samples.[21]

GC/MS analysis

The GC-MS system was equipped with (gas chromatography; Agilent 7890B) and (mass spectrometer detector; 5977A) at Central Laboratories Network, National Research Centre, Cairo, Egypt. The GC/MS assay of the petroleum ether/dichloromethane fraction was investigated by previously described method.[22] Different components were identified by the comparing the fragmentation patterns of MS spectrum with those stored in (Wiley Int. USA; NIST: Nat. Inst. St. Technol., USA), and/or the previous published data.

HPLC-ESI-MS/MS analysis

The defatted GLE was analyzed using HPLC-ESI-MS system; Thermofinnigan (Thermo electron Corporation, USA) coupled with ion trap mass spectrometer LCQ-Duo with an ESI source (ThermoQuest) according to the reported method.[23]

Statistical analysis

The values are presented as the mean ± standard error. Results were analyzed by one-way analysis of variance. When significant treatment effects were detected, Dunken-test was performed to make pair wise comparisons between individual means. Statistical analysis software SPSS 16.0 (International Business Machines, Armonk, NY, USA) was used to conduct statistical analyses. $P \leq 0.05$ was considered a statistically significant difference.

Results and Discussion

Characterization of biosynthesized AgNPs

UV-vis spectroscopic studies of the biosynthesized AgNPs

The surface plasmon resonance (SPR) band of the prepared AgNPs at the solution was formed and determined at wavelength 445-456 nm. As well as the evident for the development of AgNPs at the solution was described with the brilliant colors of dispersions AgNPs and the form of the yellowish brown color of the prepared solution. Also, the UV-vis spectra of the prepared AgNPs by mixing different concentration of GLE to definite volume of constant concentration from silver nitrate solution were demonstrated (Figure 1). It was noticed that as the increasing of *G. lotoides* concentration, the intensity of the SPR band increased and more Ag^+ ions are reduced to AgNPs.[24]

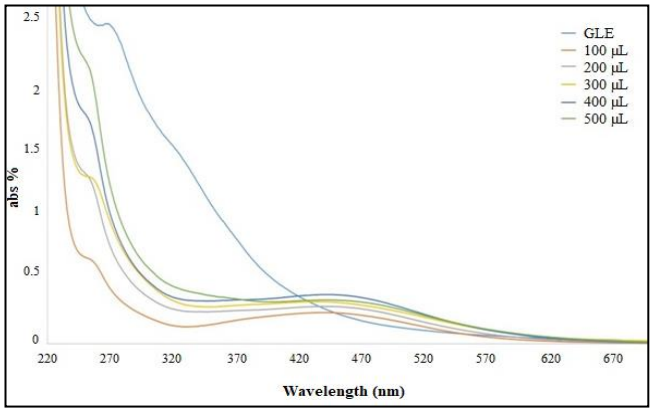

Figure 1: The SPR band of AgNPs recorded by UV-VIS spectra as a function of varying addition of GLE.

TEM studies of the bio-synthesized AgNPs

The prepared AgNPs shape and size were evaluated using the HRTEM technique (Fig. 2 A-D), which reflects the image of the particle scattering for the prepared AgNPs in the solution and the capping action of the GLE in the preparation process. The selected images of TEM illustrated that, the spherical and separated AgNPs with a significant variation in particle size between 5-50 nm (Figures 2A-D). As well as, the excess Ag^+ ions in the solution lead to the growth of the aggregation of Ag clusters structure (Figure 2A).

FTIR spectroscopic studies

The phytochemical reports of *G. lotoides* comprises of a complex mixture of phytochemicals such as sterols, flavonol-*O*-glycosides, C-

ISSN 2616-0684 (Print)
ISSN 2616-0692 (Electronic)

glycosyl flavonoids, phenolic acids, saponins and triterpenoids.[14-16] Besides, other members of the genus *Glinus* are rich with other constituents containing amino and hydroxyl groups.[25, 26] As well as, many articles recognized the reduction of the metal NPs to the existence of such functional groups. Consequently, the FTIR is a sensitive technique for decisive the functional groups responsible for the reduction of Ag NPs. FTIR spectrum of GLE exhibit a broad different IR peaks spread over the spectral range (3684−696 cm^{-1}) (Figure 3). The IR signal at 3395 cm^{-1} was assigned to the stretching vibration of (–OH) group that confirmed by CO appeared at 1075 cm^{-1}. The broadening vibration of (-CH) group at 2929 cm^{-1} of alkane was confirmed by the bending vibration of ($–CH_3$) located at 1383 cm^{-1}. Whereas the vibrational peaks at 1710 and 1619 cm^{-1} was due to the elongating vibration of aromatic (-C=O) and (–C=C) present in conjugation, respectively. The vibrational out-of-plane (oop) bending occurs at 669 cm^{-1} was assigned to the aromatic (–CH). After the interaction with $AgNO_3$, several noticeable changes on FTIR spectrum of GLE+Ag^+ were remarked. The (–OH) band was become more sharp and shifted to 3463 cm^{-1} and the appearance of (–CO) bending become weak or obscured and slightly shifted to 1131 cm^{-1}. A new stretching vibration group appeared at small split at 3354 cm^{-1} was assigned to amino group (-NH) present in protein. On the other hand, the stretching vibration of (–CH) group sharped and shifted at 2919 cm^{-1} and the bending vibration of ($–CH_3$) shifted to 1409 cm^{-1}. While, the keto group was disappeared but, the sp^2 carbon (C=C) stretch of aromatic split into two peaks and shifted into 1638 cm^{-1} and 1631 cm^{-1}.[17, 24, 27] These spectroscopic results described the reducing power of hydroxyl and amino groups present within the GLE and caused obvious shifts in the peaks frequencies.

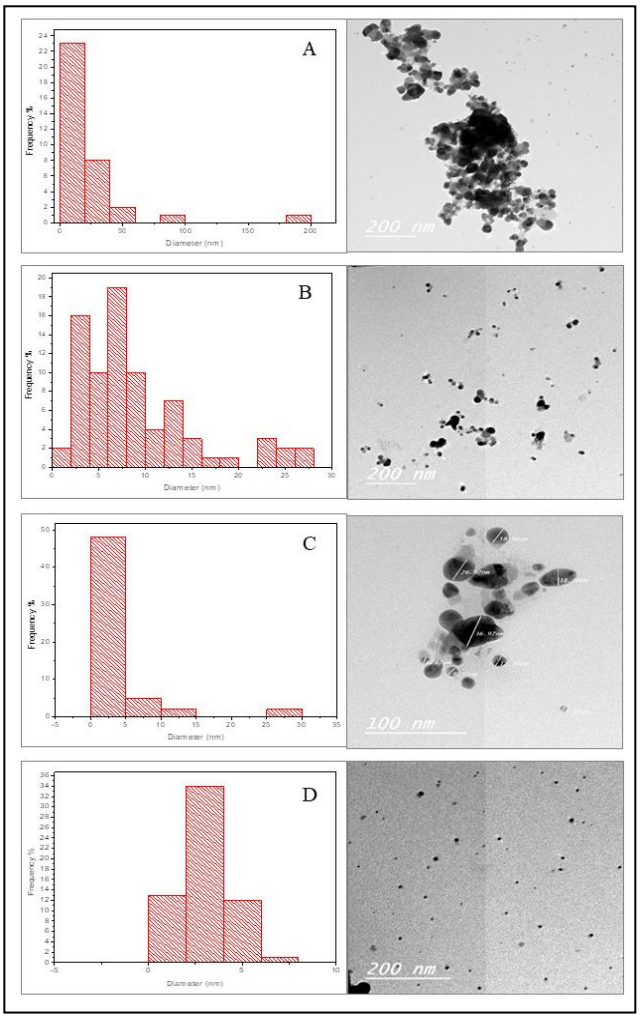

Figure 2: The TEM images of plant stabilized Ag nanoparticles at 300 µL.

In vitro cytotoxic activity of GLE and AgNPs

The GLE exhibited antiproliferative activity against the cell lines: HepG2, HCT116, MCF7 and Hep2 with IC_{50} 25.4, 26.1, 30, and 50µg/mL, respectively (Table 1). These activities could be ascribed to the existence of its fatty acids and/or phenolics. AgNPs was investigated against HepG2 and HCT116 cell lines which gave the highest antiproliferative activity and it was noticed that there is no remarkable change in its activity about IC_{50} 24.3 and 26.4, respectively. In addition, the AgNPs has no cytotoxic activity against normal human melanocytes (HFB-4). The American National Cancer Institute assigns a significant cytotoxic effect of extract for future bio guided studies if it exerts an IC_{50} value <30 µg/mL.[28]

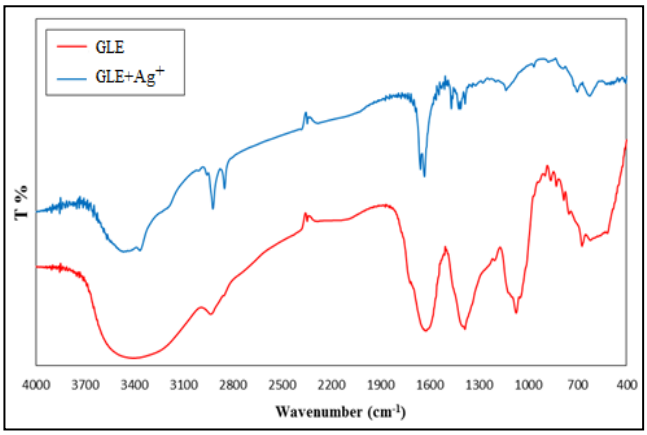

Figure 3: FTIR spectrum of GLE_AgNPs as compared with that of GLE.

In vitro antiviral activity of GLE and AgNPs

The obtained results exhibited that the GLE_AgNPs was more effective (60% virus inhibition) than GLE (26.5% virus inhibition) at 100 µg/µL. This activity may be attributed to the effective interactions of viruses with metal nanoparticles. Since the metal nanoparticles showed promising antiviral agents against HIV-1, respiratory syncytial virus, hepatitis B virus, herpes simplex virus; type 1 and influenza virus.[29] The constituent functional groups of plant extract play an important role on both the remarkable viral inhibition results and the reduction of Ag^+ to Ag^0 as stabilizing and capping agents.[30] As the functional groups increased, the rate of reduction process becomes faster and *vice versa*. Moreover, the size, the flow rate and penetration of nanoparticles to the target cells and the route of administration must be taken into account during the designed to generate optimal therapeutic effects.

On the other hand, the potential of anti-viral candidates based on plant extracts can be explained as (*i*) blocking viral entry, (*ii*) disrupting the viral replication, transcription and translation, (*iii*) impeding the nuclear export of NP, (*iv*) targeting at viral assembly, packing and budding and (*v*) host response (i.e. innate immune response and the adaptation). In addition, the second mechanism showed the reduction of the influenza-associated complications *via* synergism between the multiple drug combinations.[31] Therefore, the observed significant antiviral results of GLE could be back to their phytoconstituents, and so, it subjected to the phytochemical studies.

Phytochemical analysis

Acid hydrolysis

The paper chromatography (PC) of the ethyl acetate fraction gave five spots with the color reaction and R_f values as kaempferol, quercetin and isorhamnetin (as major aglycones, CO-PC, UV and ^{1}HNMR) as well as myricetin and diosmetin (as minor aglycones, CO-PC). In addition to, other two deep purple spots (unchanged after hydrolysis) indicated the *C*-glycoside structure and have PC properties as isoorientin and luteolin 6, 8 di-*C*-glucoside. [32,33] Glucose (major) and xylose (trace) were detected as sugar moieties in the aqueous extract.

ISSN 2616-0684 (Print)
ISSN 2616-0692 (Electronic)

Table 1: Effect of GLE and GLE_AgNPs on the % viability of different cell lines and their IC_{50}

Cell line	Sample	Concentration (ug/mL)					IC_{50}
		0	5	12.5	25	50	
HEPG-2	GLE	100 ± 0.00^{a}	85.8 ± 0.36^{b}	61.9 ± 0.41^{c}	46.8 ± 0.47^{d}	49.8 ± 0.28^{e}	25.4 ± 0.47
	GLE_AgNPs	100 ± 0.00^{a}	88.9 ± 0.408^{b}	75.6 ± 0.31^{c}	48.9 ± 0.40^{d}	40 ± 0.55^{e}	24.3 ± 0.37
	Doxorubcin	100 ± 0.00^{a}	41.9 ± 0.23^{b}	35.5 ± 0.31^{c}	33.8 ± 0.53^{d}	27.6 ± 0.30^{e}	4.28 ± 0.30
HCT-116	GLE	100 ± 0.00^{a}	80.8 ± 0.70^{b}	65.6 ± 0.46^{c}	51.2 ± 0.42^{d}	36.4 ± 0.44^{e}	26.1 ± 0.44
	GLE_AgNPs	100 ± 0.00^{a}	88.42 ± 0.23^{b}	76.69 ± 0.14^{c}	48.16 ± 0.32^{c}	34.17 ± 0.32^{e}	26.4 ± 0.27
	Doxorubcin	100 ± 0.00^{a}	35.38 ± 0.37^{b}	27.8 ± 0.60^{c}	24.41 ± 0.49^{d}	27.77 ± 0.70^{c}	3.73 ± 0.45
MCF-7	GLE	100 ± 0.00^{a}	77.4 ± 0.32^{b}	73.9 ± 0.21^{c}	55.2 ± 0.39^{d}	30.4 ± 0.30^{e}	30 ± 40
	Doxorubcin	100 ± 0.00^{a}	46.6 ± 0.21^{b}	46.4 ± 0.43^{b}	42.3 ± 0.36^{c}	43.9 ± 0.17^{d}	4.43 ± 0.28
HEP-2	GLE	100 ± 0.00^{a}	90.9 ± 0.208^{b}	83.2 ± 0.345^{c}	81.8 ± 0.15^{d}	50 ± 0.38^{e}	50 ± 0.46
	Doxorubcin	100 ± 0.00^{a}	34.32 ± 0.33^{b}	28.69 ± 0.164^{c}	22.17 ± 0.36^{d}	27.1 ± 0.313^{e}	3.73 ± 0.35
HFB-4 (normal)	GLE_AgNPs	100 ± 0.00^{a}	92 ± 0.33^{b}	89.6 ± 0.37^{c}	69.4 ± 0.51^{d}	53.5 ± 0.27^{e}	>70 ± 0.54

Data are represented as mean ± SD, n = 3, Mean values in the same column bearing the same superscript do not differ significantly ($P \leq 0.05$)

GC/MS analysis

Phytochemical investigation of the petroleum ether/dichloromethane fraction of *G. lotoides* was analyzed using GC/MS investigation and revealed the identification of 33 compounds amounting for 82.20% of the total matter (Table 2). The detected classes were saturated fatty acids (44.68%), unsaturated fatty acid (13.88%), fatty acid ester (8.42%), sterol (4.59%) and other compounds belonging to different classes (10.63%). *n*-Hexadecanoic acid (palmitic acid) constitutes the major percentage 36.02% followed by *cis*-11-Octadecenoic acid (*cis*-Vaccenic acid) 6.01% which is one of the double-bond positional isomers of oleic acid and *trans*-9, 12-Octadecadienoic acid (*trans*-linoleic acid) 5.14%.

Table 2: Results of GC/MS analysis of the petroleum ether/dichloromethane fraction of *G. lotoides*

No.	Compounds	R_t	R_{rt}	BP	M+	Molecular formula	Area %
1	Phenyl -propanedioic acid	9.76	0.45	91	180	$C_9H_8O_4$	0.35
2	Dodecanoic acid (lauric acid)	15.28	0.706	73	200	$C_{12}H_{24}O_2$	0.69
3	*trans*-13-octadecenoic acid	15.71	0.725	55	282	$C_{18}H_{34}O_2$	0.42
4	*cis*-9-Hexadecenoic acid (Palmitoleic acid)	17.11	0.79	55	254	$C_{16}H_{30}O_2$	0.7
5	2-Cyclohexen-1-one,4-(3-hydroxybutyl)-3,5,5-trimethyl-	17.64	0.814	135	210	$C_{13}H_{22}O_2$	0.73
6	Dihydroxanthin	18.28	0.844	178	308	$C_{17}H_{24}O_5$	0.73
7	Tetradecanoic acid (Myristic acid)	18.46	0.852	73	228	$C_{14}H_{28}O_2$	2.32
8	Phytol, acetate	19.52	0.901	68	278	$C_{22}H_{42}O_2$	0.71
9	6,10,14-trimethyl- 2-Pentadecanone	19.61	0.905	58	250	$C_{18}H_{36}O$	0.91
10	Pentadecanoic acid	19.89	9.18	73	242	$C_{15}H_{30}O_2$	0.96
11	Phthalic acid, butyl tetradecyl ester	19.99	0.923	149	418	$C_{26}H_{42}O_4$	0.44
12	Methyl 11-(3-pentyl-2-oxiranyl)-undecanoate.(3-Pentyl -*trans*-oxiraneundecanoic acid methyl ester)	20.57	0.95	55	312	$C_{19}H_{36}O_3$	0.27
13	2-Hexadecanol	20.62	0.952	55	242	$C_{16}H_{34}O$	0.19
14	Hexadecanoic acid methyl ester (Palmitic acid, methyl ester)	20.78	0.959	74	270	$C_{17}H_{34}O_2$	4.83
15	*cis* -9-Octadecenoic acid (*cis* -Oleic acid)	21.08	0.973	55	294	$C_{18}H_{34}O_2$	0.93
16	n-Hexadecanoic acid (Palmitic acid)	21.32	1	73	256	$C_{16}H_{32}O_2$	36.02
17	Heptadecanoic acid (Margaric acid)	22.7	1.048	73	270	$C_{17}H_{34}O_2$	0.65
18	*cis*-9,12-Octadecadienoic acid (linoleic acid)	23.07	1.065	67	292	$C_{18}H_{32}O_2$	0.68
19	10-Octadecenoic acid, methyl ester	23.15	1.069	55	296	$C_{19}H_{36}O_2$	1.55
20	16-Methyl -heptadecanoic acid methyl ester (Methyl isostearate)	23.48	1.084	74	298	$C_{19}H_{38}O_2$	0.85
21	*trans*, 9,12-Octadecadienoic acid (*trans* - linoleic acid)	23.73	1.096	67	280	$C_{18}H_{32}O_2$	5.14
22	*cis*-11-Octadecenoic acid (*cis*-Vaccenic acid)	23.81	1.099	55	282	$C_{18}H_{34}O_2$	6.01
23	Octadecanoic acid (Stearic acid)	24.08	1.112	73	284	$C_{18}H_{36}O_2$	4.04
24	*cis*-3-octyl-Oxiraneoctanoic acid (*cis*-9,10-Epoxyoctadecanoic acid)	24.573	1.121	55	298	$C_{18}H_{34}O_3$	0.15
25	*trans*- 9,12-Octadecadienoic acid ethyl ester (Ethyl linolelaidate).	24.774	1.144	67	308	$C_{20}H_{36}O_2$	0.92
26	1-Heptatriacotanol	25.952	1.189	43	536	$C_{37}H_{76}O$	0.24
27	7-Methyl-Z-tetradecen-1-ol- acetate	26.302	1.214	99	268	$C_{17}H_{32}O_2$	0.81
28	Di-isooctyl phthalate	28.51	1.316	149	390	$C_{24}H_{38}O_4$	4.96
29	3β -Stigmast-5-en-3-ol	32.962	1.522	207	414	$C_{29}H_{50}O$	0.57
30	9,19-Cyclochloestene-3,7-diol, 4,14-dimethyl-, 3-acetate	33.82	1.562	394	472	$C_{31}H_{52}O_3$	1.13
31	Cholest-5-en-3-ol (3β)	34.249	1.581	207	386	$C_{27}H_{46}O$	0.72
32	Ethyl iso-allocholate	35.314	1.631	207	436	$C_{26}H_{44}O$	0.41
33	Stigmasterol	35.669	1.647	57	412	$C_{29}H_{48}O$	2.17
	Total identified mater						82.20
	Non identified						17.80

ISSN 2616-0684 (Print)
ISSN 2616-0692 (Electronic)

The GC/MS investigation detected some active constituents which are responsible for many biological activities including cytotoxic and antiviral effects. Fatty acids have a potent impact on the health status; it is involved in different biological processes as cell membrane structure and immune responses. It was reported that administration of fatty acids in mammals improves the resistance to bacterial and viral pathogens through decreasing the microbial loads. [34-37] *n*-Hexadecanoic acid; the highest percentage in the constituents of the petroleum ether/dichloromethane fraction (36.02%, palmitic acid) is also the common fatty acid found in many plant species[38] and exhibited selectively towards proliferation of human fibroblast cells through inhibition of DNA topoisomerase-I [39].It was also reported earlier for its antioxidant, anti-inflammatory effects, pesticide and other activities. [40,41] *trans*, 9, 12-Octadecadienoic acid (*trans*- linoleic acid) was reported to have anti-carcinogenic, diabetic, atherogenic and lean body mass-enhancing properties.[42] Also, palmitic acid methyl ester (4.83%) has antifungal and antibacterial activities. [43] Additionally, octadecanoic acid (stearic acid) acts as 5-α reductase inhibitor, hypo cholesterolemic and softening agent. So most of the constituents of the petroleumether/dichloromethane fraction were reported for various biological activities which might be improve the traditional medicines of the plant.

HPLC-ESI-MS/MS analysis

HPLC-ESI-MS/MS analysis (full scan and product ion scan mode) has providing complete structural information and effectively directed to the characterization and identification of 30 metabolites, including 21 flavonoids (Table 3 and Figure 4).

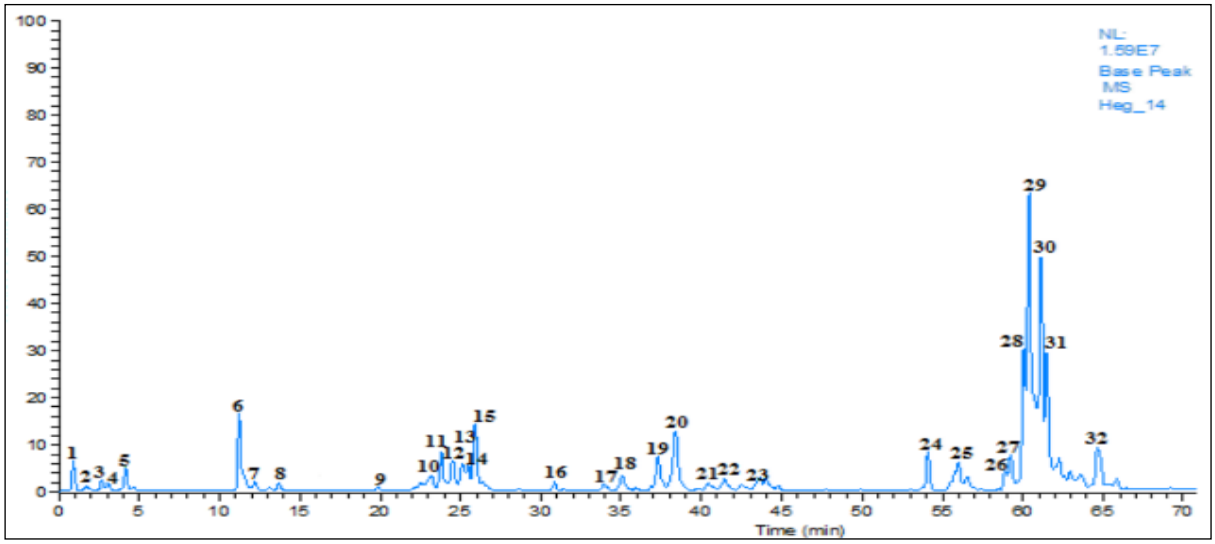

Figure 4: Base peak chromatogram of the defatted GLE.

Peak (**1**) was tentatively characterized as galloyl phthalic acid. This assignment is based on its [M-H]$^-$ ion (*m/z* 317) and released fragments at *m/z* 165 and *m/z* 121 represented to the phthalic moiety structure. It may be involved and connected with galloyl moiety which categorized with the other fragments at *m/z* 169, 153 and 125.[44, 45] Furthermore, peak (**2**) exposed an [M-H]$^-$ ion at *m/z* 290 and fragmented to *m/z* 272, 199, 133 and 115, these fragmentations pattern were similar to a malic acid derivative. Peak (**3**) showed a molecular ion (*m/z* 175) and product ions (*m/z* 157, 131, 115) similar to ascorbic acid which was identified previously in the leaves of *G. lotoides*.[45] Based on the MS data and previous literature, peak (**4**) (*m/z* 321) is assigned as digallic acid[46] and peak **5** (*m/z* 305) is tentatively identified as gallocatechin.[23] Peak (**6**) showed a molecular ion [M-H]$^-$ at *m/z* 289 and yielding a fragment at *m/z* 221 and is identified as catechin which was identified before in the leaves of *G. lotoides*. [47] On the basis of acid hydrolysis, the tri-*O*-glucosides of quercetin (*m/z* 301) and kaempferol (*m/z* 285) were shown in peak (**7**) and (**8**) with [M-H]$^-$ ions at *m/z* 787 and 771, respectively. Their tentative identification was confirmed by loss of one glucose moiety assigned at (*m/z* 625 and 609), and then loss of the two other glucose moieties revealed the quercetin and kaempferol ions. [48] Peaks (**9**) and (**20**) with molecular ions at *m/z* 609 and 447 are showed fragmentations pattern of *C*-hexosyl flavone structure, confirmed by the loss of (-90 amu) and (-120 amu).[49] Compound (**9**) exhibited fragment ions at *m/z* 489 [M-120-H]$^-$, and *m/z* 519 [M-90-H]$^-$, while compound (**20**) at *m/z* 327 [M-120-H]$^-$ and *m/z* 357 [M-90-H]. Respectively, they were assigned as luteolin 6,8-di-*C*-glucoside and luteolin 6-*C*-glucoside (isoorientin), maintained by CO-PC after acid hydrolysis. [32] Compound **(10)** showed [M-H]$^-$ ion at *m/z* 977 and gave a fragment ion at *m/z* 801 [M-H-176]$^-$, after loss of either acyl moiety (feruloyl) or glycosyl moiety (glucuronoic acid or galacturonic acid). Herein the substitution group is feruloyl one, confirmed by the presence of an additional fragment ion at *m/z* 787 [M-H-(feruloyl+CH_2)]$^-$, loss of 14 Da higher than the loss of the acyl group, matching to the loss of the acyl neglected of the methyl group.[49] Other fragments were observed at *m/z* 639 [M-H-feruloyl glucoside]$^-$ and 315 [M-H-feruloyl tri-glucoside]$^-$, confirmed by loss of one glucose moiety, then loss of two other glucose moieties, suggested the tentative identification of isorhamnetin feruloyl tri-*O*-glucoside. Peaks (**11** and **15**) at [M-H]$^-$ ions (*m/z* 963 and 947) showed typical fragments of compounds **7** and **8** (*m/z* 787 and 771) [M-H-176]$^-$, respectively, with an extra 176 amu, suggestive for the substitution with feruloyl moiety confirming by the presence of fragment ions at *m/z* 773 and 757 [M-H-(acyl+14)]$^-$ for **11, 15**, respectively.[49] Therefore, **11** and **15** were considered as feruloyl tri-*O*-glucoside of quercetin and kaempferol. [50] Peaks (**12**) and (**13**) at *m/z* 947 and 949 have the same substitution of diosmetin and quercetin, respectively (evidence by acid hydrolysis). They gave fragment ions at *m/z* 785 and 787 [M-H-162]$^-$, after loss of a caffeoyl moiety. Other fragment was observed at *m/z* 341 [caffeoyl glucoside-H]$^-$confirmed its attachment to the same OH group and the two other diglucose moiety to other OH group of the aglycone. Thus (**12**) and (**13**) were tentatively identified as diosmetin-*O*-caffeoyl glucoside-*O*-diglucoside and quercetin-*O*-caffeoyl glucoside-*O*-diglucoside, [49] respectively. Peak (**14**) at *m/z* 949 gave fragment ions at *m/z* 803 [M-H-146]$^-$, after loss of a coumaroyl moiety and *m/z* 625 by losing the glucose unit. Other fragment was observed at *m/z* 317 after loss of a diglucoside residue and corresponding to a myricetin aglycone, therefore compound (**14**) was tentatively identified as myricetin-*O*-coumaroylglucoside-*O*-diglucoside.[49] Compound (**16**) showed a molecular ion peak at *m/z* 163 [M-H]$^-$ and a product ion *m/z* 119 after the loss of CO_2 residue, indicating the presence of coumaric acid structure. Peak (**17**) at *m/z* 801 [M-H]$^-$ gave fragments at *m/z* 639 [M-

ISSN 2616-0684 (Print)
ISSN 2616-0692 (Electronic)

H-caffeoyl]$^-$ and *m/z* 315 [M-H-caffeoyl diglucoside]$^-$ suggested the characterization of isorhamnetin *O*-caffeoyl diglucoside. The identification was supported by the occurrence of a fragment at *m/z* 503 which represented as a caffeoyl diglucoside residue. Compounds (**18** and **19**) at *m/z* 801 and 785 seemed likely those derivatives of (**11** and **15**) lacking the-*O*-glucosyl substitution. Thus, they were characterized as feruloyl di-*O*-glucoside of quercetin and kaempferol, respectively. Likewise, compound **32** (*m/z* 623) is a feruloyl mono glycoside of kaempferol and showed product ions at 433 [M-H-(feruloyl+14)]$^-$ and 285 [kaempferol-H]$^-$. Peaks (**21**) at *m/z* 963 gave fragment ions at *m/z* 639 [M-H-324]$^-$ and 625 [M-H-338], after loss of a caffeoyl moiety and feruloyl hexoside. Other fragment was observed at *m/z* 341 [caffeoyl glucoside-H]$^-$ and *m/z* 355 [feruloyl glucoside-H]$^-$, confirmed that caffeoyl glucoside and feruloyl glucoside were attached to two different hydroxyl group of the aglycone. In addition to, a fragment at *m/z* 301, suggested the quercetin aglycone. Thus (**21**) was tentatively identified as quercetin-*O*-caffeoyl glucoside-*O*-feruloyl glucoside. Peak (**22**) has similar molecular ion peak and fragmentation patterns of compound (**18**), suggested that (**22**) is another isomer of quercetin feruloyl tri-*O*-glucoside. Peak (**23**) (*m/z* 595) with MS fragments at *m/z* 433 (loss of 162) and 301 (loss of 132), suggesting that it might be a quercetin diglycoside containing glucose and xylose moieties (evidence by acid hydrolysis). No MS fragment was detected at *m/z* 463 which established that both sugar moieties were linked to the same phenolic hydroxyl as a disaccharide residue. Moreover, the presence of *m/z* 433 (loss of glucose) then at 301 (loss of xylose) could be suggested that the glucose moiety is in a terminal position, while the xylose one is directly attached to the aglycone (glucosyl xyloside).[51] Therefore, peak **23** was tentatively identified as *O*-glucosyl xyloside of quercetin. A flavonol mono glucoside was shown in the MS of peak **27** (*m/z* 479) and produce a fragment ion at *m/z* 317, after the loss of glucose moiety, supporting the existence of myricetin *O*-glucoside. Peaks (**29**, **30** and **31**) revealed molecular ion peaks at *m/z* (317, 301 and 299) and were corresponding to myricetin, quercetin and diosmetin, respectively, confirmed by the acid hydrolysis. In accordance with reported literature, peak (**24**) was tentatively identified as tetrahydroxy-octadecenoic acid, [52] while peak (**25**) was suggested to be trihydroxyoctadecenoic acid.[53]

Table 3: Chemical composition of defatted GLE using LC-MS/MS

No.	t_R(min)	[M-H]$^-$	*m/z* fragments [Ms^2]	Tentatively identified compound
1	0.93	317	169,165, 153, 125, 121	Galloyl phthalic acid
2	1.73	290	272, 199, 133, 115	Malic acid derivative
3	2.86	175	157, 131, 115, 85	Ascorbic acid
4	3.03	321	169, 97	Digallic acid
5	4.15	305	287, 225, 169, 97	Gallocatechin
6	11.22	289	289, 245, 221, 97	Catechin
7	12.18	787	625, 301	Quercetin-tri-*O*-glucoside
8	13.69	771	609, 285	Kaempferol-tri-*O*-glucoside
9	19.84	609	519, 489, 447, 327, 285	Luteolin 6,8 -di-*C*-glucoside*
10	23.15	977	801, 787, 639, 315	Isorhamnetin *O*-feruloyl tri-glucoside
11	23.79	963	787, 773, 625, 301	Quercetin *O*-feruloyl tri-glucoside
12	24.14	947	785, 623, 341, 299	Diosmetin *O*-caffeoyl glucoside-*O*-diglucoside
13	25.13	949	787,625, 341,301, 299	Quercetin *O*-caffeoyl glucoside-*O*-diglucoside
14	25.47	949	803, 641,625 , 325, 317	Myricetin *O*-coumaroyl glucoside-*O*-diglucoside
15	25.89	947	771,757, 609, 285	kaempferol *O*- feruloyl tri-glucoside
16	30.84	163	119	Coumaric acid
17	33.93	801	639, 503, 315	Isorhamnetin *O*-caffeoyl diglucoside
18	35.05	801	625, 611, 301	Quercetin *O*- feruloyl di-glucoside
19	37.27	785	623, 609, 461, 447, 285	Kaempferol *O*- feruloyl di-glucoside
20	38.37	447	357, 327	Luteolin 6-*C*-glucoside (isoorientin)*
21	40.38	963	639, 625, 355, 341, 301	Quercetin *O*-caffeoyl glucoside-*O*-feruloyl glucoside
22	41.41	963	801, 787, 625,301	Quercetin *O*-feruloyl triglucoside
23	43.99	595	433, 301, 300, 299	Quercetin *O*-glucosyl xyloside
24	54.09	345	327, 309, 301, 225	Tetrahydroxy-octadecenoic acid
25	55.98	329	329, 311, 229, 301	Trihydroxy-octadecenoic acid
26	58.92	555	343,129	NI
27	59.25	479	317, 299, 256, 243, 225	Myricetin *O*-glucoside
28	60.03	317	299	NI
29	60.3	317	299, 258, 243	Myricetin*
30	61.1	301	300,299,225	Quercetin*
31	61.49	299	285, 225	Diosmetin*
32	64.65	623	623, 433, 285	Kaempferol-*O*- feruloyl glucoside

*; Reference samples, NI; Non Identified.

Conclusions

This study is paying attention to the possibility for synthesizing AgNPs using natural biomolecules *via* a simple and eco-friendly green approach which could be used in pharmaceutical industry. AgNPs synthesized from *G. lotoides* showed a significant antiviral activity. Additionally, the studying of the chemical contents of *G. lotoides;* an important edible plant; revealed the detection and characterization of around sixty metabolites for the first time.

Conflict of interest

The authors have no conflict of interest.

Authors' Declaration

The authors hereby declare that the work presented in this article is original and that any liability for claims relating to the content of this article will be borne by them.

Acknowledgments

The authors are grateful to Dr. M. Sobeh (IPMB), Universität Heidelberg, for gathering HPLC-MS/MS data. The authors are also wish to thank Center of Scientific Excellence for Influenza Viruses, National Research Centre, Dokki, Egypt for antiviral studies.

References

1. Haggag EG, Elshamy AM, Rabeh MA, Gabr NM, Salem M, Youssif KA, Samir A, Muhsinah AB, Alsayari A, Abdelmohsen UR. Antiviral potential of green synthesized silver nanoparticles of *Lampranthus coccineus* and *Malephora lutea*. Int J Nanomed. 2019; 14:6217.
2. Ajitha B, Reddy YAK, Reddy PS. Biosynthesis of silver nanoparticles using *Plectranthus amboinicus* leaf extract and its antimicrobial activity. Spectrochim Acta A Mol Biomol Spectrosc. 2014; 128:257-262.
3. Kathiravan V, Ravi S, Ashokkumar S, Velmurugan S, Elumalai K, Khatiwada CP. Green synthesis of silver nanoparticles using *Croton sparsiflorus* morong leaf extract and their antibacterial and antifungal activities. Spectrochim Acta A Mol Biomol Spectrosc. 2015; 139:200-205.
4. Švecová M, Ulbrich P, Dendisová M, Matějka P. SERS study of riboflavin on green-synthesized silver nanoparticles prepared by reduction using different flavonoids: What is the role of flavonoid used?. Spectrochim Acta A Mol Biomol Spectrosc. 2018; 195:236-245.
5. Esawy MA, Ragab TI, Basha M, Emam M. Evaluated bioactive component extracted from *Punica granatum* peel and its Ag NPs forms as mouthwash against dental plaque. Biocatal Agric Biotechnol. 2019; 18:101073.
6. Ragab TI, Nada AA, Ali EA, Soliman AA, Emam M, El Raey MA. Soft hydrogel based on modified chitosan containing *P. granatum* peel extract and its nano-forms: Multiparticulate study on chronic wounds treatment. Int J Biol Macromol. 2019; 135:407-421.
7. El-Rafie HM and Hamed MAA. Antioxidant and anti-inflammatory activities of silver nanoparticles biosynthesized from aqueous leaves extracts of four *Terminalia* species. Adv Nat Sci: Nanosci Nanotechnol. 2014; 5:035008.
8. AshaRani P, Mun GL, Hande MP, Valiyaveettil S. Cytotoxicity and genotoxicity of silver nanoparticles in human cells. ACS Nano. 2008; 3:279-290.
9. Balakrishnan S, Sivaji I, Kandasamy S, Duraisamy S, Kumar NS, Gurusubramanian G. Biosynthesis of silver nanoparticles using *Myristica fragrans* seed (nutmeg) extract and its antibacterial activity against multidrug-resistant (MDR) Salmonella enterica serovar Typhi isolates. Environ Sci Poll Res. 2017; 24:14758-14769.
10. Lara HH, Ayala-Nuñez NV, Ixtepan-Turrent L, Rodriguez-Padilla C. Mode of antiviral action of silver nanoparticles against HIV-1. J Nanobiotechnol. 2010; 8:1.
11. Galdiero S, Falanga A, Cantisani M, Ingle A, Galdiero M, Rai M. Silver nanoparticles as novel antibacterial and antiviral agents. In handbook of nanobiomedical research*:* Fundamentals, Applications and Recent Developments. Materials for Nanomedicine, World Sci. 2014; 1:565-594.
12. Sharma V, Kaushik S, Pandit P, Dhull D, Yadav JP, Kaushik S. Green synthesis of silver nanoparticles from medicinal plants and evaluation of their antiviral potential against chikungunya virus. Appl Microbiol Biotechnol. 2019; 103:881-891.
13. Mengesha AE and Youan BBC. Anticancer activity and nutritional value of extracts of the seed of *Glinus lotoides*. J Nutr Sci Vitaminol. 2010; 56:311-318.
14. Biswas T, Gupta M, Achari B, Pal BC. Hopane-type saponins from *Glinus lotoides* Linn. Phytochem. 2005; 66:621-626.
15. Hamed AI and El-Emary NA. Triterpene saponins from *Glinus lotoides* var. dictamnoides fn1. Phytochem. 1999; 50:477-480.
16. Bhavani S. *Glinus lotoides* (Ciru-Ceruppadai): An overview. J Chem Pharm Res. 2015; 7:676-682.
17. Emam M, El Raey MA, Eisa WH, El-Haddad AE, Osman SM, El-Ansari MA, Rabie AG M. Green Synthesis of Silver Nanoparticles from *Caesalpinia gilliesii* (Hook) leaves: antimicrobial activity and *in vitro* cytotoxic effect against BJ-1 and MCF-7 cells. J Appl Pharm Sci. 2017; 7:226-233.
18. Vichai V and Kirtikara K. Sulforhodamine B colorimetric assay for cytotoxicity screening. Nat Protoc. 2006; 1:1112-1116.
19. Rashad AE, Shamroukh AH, Abdel-Megeid RE, Mostafa A, El-Shesheny R, Kandeil A, Ali MA, Banert K. Synthesis and screening of some novel fused thiophene and thienopyrimidine derivatives for anti-avian influenza virus (H5N1) activity. Eur J Med Chem. 2010; 45:5251-5257.
20. Saleme MdLS, Cesarino I, Vargas L, Kim H, Vanholme R, Goeminne G, Van Acker R, de Assis Fonseca FC, Pallidis A, Voorend W. Silencing -caffeoyl shikimate esterase affects lignification and improves saccharification. Plant Physiol. 2017; 157(3):1040-1057.
21. Marzouk MM, Hussein SR, Elkhateeb A, Farid MM, Ibrahim LF, Abdel-Hameed ESS. Phenolic profiling of *Rorippa palustris* (L.) Besser (Brassicaceae) by LC-ESI-MS: Chemosystematic significance and cytotoxic activity. Asian Pac J Trol Dis. 2016; 6:633-637.
22. Adams RP. Identification of Essential Oil Components by Gas Chromatography/Mass Spectrometry. 4th Edition Allured Publishing Corporation, Carol Stream. 2007.
23. Sobeh M, Mahmoud MF, Hasan RA, Cheng H, El-Shazly AM, Wink M. *Senna singueana*: Antioxidant, hepatoprotective, antiapoptotic properties and phytochemical profiling of a methanol bark extract. Mol. 2017; 22:1502.
24. El Raey MA, El-Hagrassi AM, Osman AF, Darwish KM, Emam M. *Acalypha wilkesiana* flowers: Phenolic profiling, cytotoxic activity of their biosynthesized silver nanoparticles and molecular docking study for its constituents as Topoisomerase-I inhibitors. Biocatal Agric Biotechnol. 2019; 20:101243.
25. Sahakitpichan P, Disadee W, Ruchirawat S, Kanchanapoom T. *L*-(-)-(*N*-trans-Cinnamoyl)-arginine, an Acylamino Acid from *Glinus oppositifolius* (L.) Aug. DC. Mol. 2010; 15:6186-6192.
26. Chhanda SA, Muslim T, Rahman MA. Phytochemical Studies on *Glinus oppositifolius* (L.) Aug. DC. Dhaka Univ J Sci. 2014; 62:45-48.
27. Eisa WH, Zayed MF, Anis B, Abbas LM, Ali SS, Mostafa AM. Clean production of powdery silver nanoparticles using *Zingiber officinale*: the structural and catalytic properties. J Clean Prod. 2019; 241:118398.
28. Suffness MP and Pezzuto JJM. Assays related to cancer drug discovery. Methods in Plant Biochemistry: Assays for Bioactivity; Hostettman, K., Ed. 1990; 6:71-133 p.
29. Elechiguerra JL, Burt JL, Morones JR, Camacho-Bragado A, Gao X, Lara HH, Yacaman MJ. Interaction of silver nanoparticles with HIV-1. J Nanobiotechnol. 2005; 3:6.
30. Prasannaraj G and Venkatachalam P. Green engineering of biomolecule-coated metallic silver nanoparticles and their potential cytotoxic activity against cancer cell lines. Advances in Natural Sciences: J Nanosci Nanotechnol. 2017; 8(2):025001.
31. Yi Tsang N, Zhao LH, Wai Tsang S, Zhang HJ. Antiviral Activity and Molecular Targets of Plant Natural Products Against Avian Influenza Virus. Curr Org Chem. 2017; 21:1777-1804.
32. Hussein SR, Latif RRA, Marzouk MM, Elkhateeb A, Mohammed RS, Soliman AA, Abdel-Hameed ESS. Spectrometric analysis, phenolics isolation and cytotoxic activity of *Stipagrostis plumosa* (Family Poaceae). Chem Papers. 2018; 72:29-37.
33. Helal M and El Negomy I. Flavonoid constituents from *Morettia philaena* (Del.) DC. and their antimicrobial activity. J Appl Sci Res. 2012; 8:1484-1489.
34. Librán-Pérez M, Pereiro P, Figueras A, Novoa B. Antiviral activity of palmitic acid via autophagic flux inhibition in *zebrafish* (Danio rerio). Fish Shellfish Immunol. 2019; 95:595-605.
35. Zhao L, Chen Y, Wu K, Yan H, Hao X, Wu Y. Application of fatty acids as antiviral agents against *tobacco mosaic* virus. Pestic Biochem Physiol. 2017; 139:87-91.

36. Svahn SL, Ulleryd MA, Grahnemo L, Ståhlman M, Borén J, Nilsson S, Jansson JO, Johansson ME. Dietary omega-3 fatty acids increase survival and decrease bacterial load in mice subjected to *Staphylococcus aureus*-induced sepsis. Infect Immun. 2016; 84:1205-1213.
37. Svahn SL, Grahnemo L, Pálsdóttir V, Nookaew I, Wendt K, Gabrielsson B, Schéle E, Benrick A, Andersson N, Nilsson S. Dietary polyunsaturated fatty acids increase survival and decrease bacterial load during septic *Staphylococcus aureus* infection and improve neutrophil function in mice. Infect Immun. 2015; 83:514-521.
38. Rustan AC and Drevon CA. Fatty acids: structures and properties. *e LS*. John Wiley & Sons, Ltd. 2001. 1-7 p.
39. Harada H, Yamashita U, Kurihara H, Fukushi E, Kawabata J, Kamei Y. Antitumor activity of palmitic acid found as a selective cytotoxic substance in a marine red alga. Anticancer Res. 2002; 22:2587.
40. Aparna V, Dileep KV, Mandal PK, Karthe P, Sadasivan C, Haridas M. Anti-inflammatory property of *n*-hexadecanoic acid: structural evidence and kinetic assessment. Chem Biol Drug Des. 2012; 80:434-439.
41. Rahuman AA, Gopalakrishnan G, Ghouse BS, Arumugam S, Himalayan B. Effect of *Feronia limonia* on mosquito larvae. Fitoter. 2000; 71:553-555.
42. Pariza MW, Park Y, Cook ME. The biologically active isomers of conjugated linoleic acid. Prog Lipid Res. 2001; 40:283-298.
43. Chandrasekaran M, Senthilkumar A, Venkatesalu V. Antibacterial and antifungal efficacy of fatty acid methyl esters from the leaves of *Sesuvium portulacastrum* L. Eur Rev Med Pharmacol Sci. 2011; 15:775-780.
44. Brent LC, Reiner JL, Dickerson RR, Sander LC. Method for characterization of low molecular weight organic acids in atmospheric aerosols using ion chromatography mass spectrometry. Anal Chem. 2014; 86:7328-7336.
45. Boonpangrak S, Lalitmanat S, Suwanwong Y, Prachayasittikul S, Prachayasittikul V. Analysis of ascorbic acid and isoascorbic acid in orange and guava fruit juices distributed in Thailand by LC-IT-MS/MS. Food Anal Meth. 2016; 9:1616-1626.
46. Abu-Reidah IM, Ali-Shtayeh MS, Jamous RM, Arráez-Román D, Segura-Carretero A. HPLC–DAD–ESI-MS/MS screening of bioactive components from *Rhus coriaria* L.(Sumac) fruits. Food Chem. 2015; 166:179-191.
47. Spínola V, Pinto J, Castilho PC. Identification and quantification of phenolic compounds of selected fruits from Madeira Island by HPLC-DAD–ESI-MSn and screening for their antioxidant activity. Food Chem. 2015; 173:14-30.
48. Elkhateeb A, El-Shabrawy M, Abdel-Rahman RF, Marzouk MM, El-Desoky AH, Abdel-Hameed ESS, Hussein SR. LC-MS-based metabolomic profiling of *Lepidium coronopus* water extract, anti-inflammatory and analgesic activities, and chemosystematic significance. Med Chem Res. 2019; 28:505-514.
49. Ferreres F, Andrade PB, Valentão P, Gil-Izquierdo A. Further knowledge on barley (*Hordeum vulgare* L.) leaves *O*-glycosyl-*C*-glycosyl flavones by liquid chromatography-UV diode-array detection-electrospray ionisation mass spectrometry. J Chromatogr A. 2008; 1182:56-64.
50. Kite GC, Rowe ER, Lewis GP, Veitch NC. Acylated flavonol tri- and tetraglycosides in the flavonoid metabolome of *Cladrastis kentukea* (Leguminosae). Phytochem. 2011; 72:372-384.
51. Ibrahim LF, Elkhateeb A, Marzouk MM, Hussein SR, Abdel-Hameed ESS, Kassem ME. Flavonoid investigation, LC–ESI-MS profile and cytotoxic activity of *Raphanus raphanistrum* L.(Brassicaceae). J Chem Pharm Res. 2016; 8:786-793.
52. Farag MA, Sakna ST, El-fiky NM, Shabana MM, Wessjohann LA. Phytochemical, antioxidant and antidiabetic evaluation of eight *Bauhinia* L. species from Egypt using UHPLC–PDA–qTOF-MS and chemometrics. Phytochem. 2015; 119:41-50.
53. Napolitano A, Cerulli A, Pizza C, Piacente S. Multi-class polar lipid profiling in fresh and roasted hazelnut (*Corylus avellana* cultivar "Tonda di Giffoni") by LC-ESI/LTQOrbitrap/MS/MSn. Food Chem. 2018; 269:125-135.